Dentomaxillofacial Radiology (2010) 39, 349–355

http://dmfr.birjournals.org

RESEARCH

Diagnosing common parotid tumours with magnetic resonance imaging including diffusion-weighted imaging *vs* fine-needle aspiration cytology: a comparative study

H Yerli*[,1], E Aydin[2], N Haberal[3], A Harman[1], T Kaskati[4] and S Alibek[5]

Departments of [1]Radiology, [2]Otolaryngology and [3]Pathology, Baskent University Faculty of Medicine, Ankara, Turkey; [4]Department of Biostatistics, Ankara University Faculty of Medicine, Ankara, Turkey; [5]Department of Radiology, Erlangen University, Erlangen, Germany

Objectives: The purpose of this study was to evaluate the accuracy of MRI combined with diffusion-weighted imaging (DWI) *vs* fine-needle aspiration cytology (FNAC) in diagnosing common parotid masses.
Methods: 25 consecutive patients (mean age 61 years) with parotid masses were included in this study. Informed consent and ethical approval was obtained. 22 patients underwent both MRI combined with DWI and FNAC. From DWI data, apparent diffusion coefficient maps were generated. The MRI study protocol consisted of T_1 weighted spin echo; T_2 weighted and T_2 weighted fat-suppressed turbo spin echo; DWI; and T_1 weighted fat-suppressed post-contrast images. MRI and FNAC diagnoses were compared with histopathology. Youden's index was used to compare the two methods.
Results: Masses comprised eight Warthin tumours, eight adenomas (six pleomorphic adenomas, two basal cell adenomas), five carcinomas, two lipomas, one haemagioma and one benign lymphadenopathy. Technically, MRI was successful in 24 of the 25 patients (96%), FNAC was successful in 20 of the 23 patients (87.0%). The accuracy, sensitivity and specificity of MRI without DWI were 96%, 80% and 100%, respectively. Diagnostic accuracy did not increase by adding DWI to conventional MRI; however, DWI was helpful for diagnosing benign tumour histology. MRI combined with DWI was successful for determining accurate tumour typing in all benign masses except one lymphadenopathy. When FNAC had adequate material the accuracy, sensitivity and specificity were 95%, 75% and 100%, respectively. Youden's index was 0.80 for MRI and 0.75 for FNAC.
Conclusions: MRI combined with DWI seems to have similar diagnostic potential as FNAC in differentiation of benign *vs* malignant parotid masses.
Dentomaxillofacial Radiology (2010) **39,** 349–355. doi: 10.1259/dmfr/15047967

Keywords: magnetic resonance; diffusion study; parotid neoplasms; fine-needle aspiration cytology

Introduction

MRI and fine-needle aspiration cytology (FNAC) are widely used methods for evaluation of parotid gland masses and surgical planning. MRI indicates the deep or superficial location of the parotid gland mass, as well as any additional mass that cannot be determined by physical examination, tumour extension, tumour contour, signal features, and the relation between the tumour and the facial nerve. Apparent diffusion coefficient (ADC) values calculated from diffusion-weighted imaging (DWI) data provide additional quantitative information related to random diffusion of water molecules in tissues and functionally complement conventional MRI.[1–4] Fine-needle aspiration cytology, which provides a cytological diagnosis, is a minimally invasive and easy to perform diagnostic procedure; however, the most significant problem with FNAC is that the procedure frequently

*Correspondence to: Dr Hasan Yerli, Assistant Professor of Radiology, Baskent University Zubeyde Hanim, Practice and Research Center, Department of Radiology, 6371 Sk. No. 34 Bostanli/Karsiyaka, Izmir, Turkey, 35590; E-mail: hasanyerli@yahoo.com
Received 19 May 2009; revised 3 August 2009; accepted 16 August 2009

obtains inadequate material, thus making evaluation impossible[5,6].

To the authors' knowledge, the ability of MRI combined with DWI and of FNAC to diagnose common parotid masses has not been compared. In this study the accuracy of MRI combined with DWI is evaluated and compared with that of FNAC in diagnosing common parotid masses. The diagnostic accuracy of both methods was compared with histopathological results obtained from surgical specimens, which served as the gold standard.

Materials and methods

Patients

25 consecutive patients (16 women, 9 men, aged 31 to 90 years, mean age 61 years) with parotid masses were included in the study over a period of 2 years. MRI could not be performed in one patient who had cervical osteoarthritis. FNAC could not be performed in one patient whose parotid tumour was in the parapharyngeal area. One patient with facial nerve paralysis had a mass that showed perineural extension on MRI examination. This patient underwent surgery without FNAC. In total, 22 patients were assessed with both MRI combined with DWI, and FNAC. The project was approved by the ethics committee of Baskent University hospital, and informed consent was obtained from all patients.

MRI and DWI

MRI examinations were performed with a 1.5-T system (MAGNETOM Symphony; Siemens Healthcare, Erlangen, Germany) using a phased-array head and neck coil. MRI protocol consisted of T_1 weighted (T1W) spin-echo (SE) (time to repeat /time to echo (TR/TE): 500/14 ms), T_2 weighted (T2W) turbo SE (TR/TE: 3800–4140/90 ms) and fat-suppressed T2W sequences (TR/TE: 4120–4160/90 ms) in the axial plane with 5-mm slice thickness. DWI was performed with an echoplanar SE sequence (TR/TE, 3400/94 ms; field of view, 160 × 160 mm; matrix, 128 × 128; excitations, 5; and slice thickness, 5 mm) in the axial plane with three different *b*-values (0, 500 and 1 000 $mm^2 s^{-1}$). Acquisition time for DW MRI was 1 min 40 s. Finally, axial, coronal and sagittal fat-saturated T1W SE sequences were obtained after a body weight-adapted injection of 0.1 $mmol\,kg^{-1}$ of gadopentetate dimeglumine (Magnevist, Bayer Schering Pharma, Berlin, Germany). The ADC of each mass was measured using a circular region of interest. Measurements were performed in solid tumour components and cystic–necrotic parts were excluded from measurements.

For conventional MRI readings, criteria from the literature, for diagnosing parotid gland masses were used.[3,4,7–12] Round or lobulated, well-defined contours, low-intensity rims representing a capsule, homogeneous hyperintense signal intensity on T2W images and multinodular enhancement were accepted as benign mass characteristics. Masses matching these criteria with ADC values greater than 1.3×10^{-3} $mm^2 s^{-1}$ were diagnosed as adenomas and masses with ADC values lower than 1.1×10^{-3} $mm^2 s^{-1}$ as Warthin tumours[7]. Masses showing homogeneous hyperintense signal intensity on both T1W and T2W images and low signal of fat with fat-suppressed T2W images were diagnosed as lipomas. Masses showing focal signal voids were diagnosed as haemangiomas. Irregular tumour margins, invasion into adjacent structures, heterogeneous hypointense signal intensity on T2W images and intermediate ADC values between $1.1–1.3 \times 10^{-3}$ $mm^2 s^{-1}$ were accepted as malignant mass features.[7,13] All MRI scans were evaluated by two radiologists in consensus, both of them with over 5 year experience in the field of head and neck radiology.

FNAC

All FNAC procedures were performed under ultrasound guidance (Hitachi, EUB 6500; Hitachi Medical Systems (S) Pte Ltd, Singapore) by two interventional radiologists, both with over 5 years of experience in FNAC. A 22G needle was used and at least two needle passes were performed. The material obtained was spread on microscopic slides with approximately 10 slides prepared for each aspiration. Air-dried and alcohol-fixed smears were stained with May–Grünwald–Giemsa and with haematoxylin/eosin. All FNAC diagnoses were made by the same pathologist with 5 years of experience in FNAC.

Histopathological diagnosis

All patients underwent parotid mass surgery and, after complete excision, histopathological diagnosis of the surgical specimens was obtained and used as the gold standard diagnosis. Diagnosis of MRI DWI and FNAC were then compared.

Statistical analysis

Youden's index (Y = sensitivity + specificity − 1) was used to compare the diagnostic performance of both of the pre-operative methods. Differences among the ADC values for Warthin tumours, adenomas and carcinomas were assessed using Kruskal–Wallis variance analysis. A multiple comparison test was then performed to determine which groups differed from each other.[14]

Results

Masses

Histological diagnoses found adenoma in eight cases (six of these were pleomorphic adenomas (Figure 1) and two were basal cell adenomas), Warthin tumour in eight cases (Figure 2), carcinoma in five cases (three of which were adenoid cystic carcinomas and two which were adenocarcinomas (Figure 3)), lipoma in two cases, haemangioma in one case and benign lymphadenopathy in one case. The mass diameter ranged from 12 to

25 mm on the short axis (mean, 16.2 mm) and from 16 to 40 mm on the long axis (mean, 23.4 mm).

MRI and DWI findings

In 24 of 25 patients (96%) MRI examination was technically successful; one patient could not remain in the appropriate scan position because of cervical osteoarthritis. None of the patients had any adverse reaction to the injected contrast material. Irregular tumour margins and heterogeneous hypointense signal on T2W images were helpful in diagnosing malignant parotid masses (Figure 3a). Four out of five carcinomas (80%) showed irregular contours on MRI. Three out of five carcinomas (60%) had heterogeneous hypointense signal intensity on T2W images. One adenoid cystic carcinoma, which had

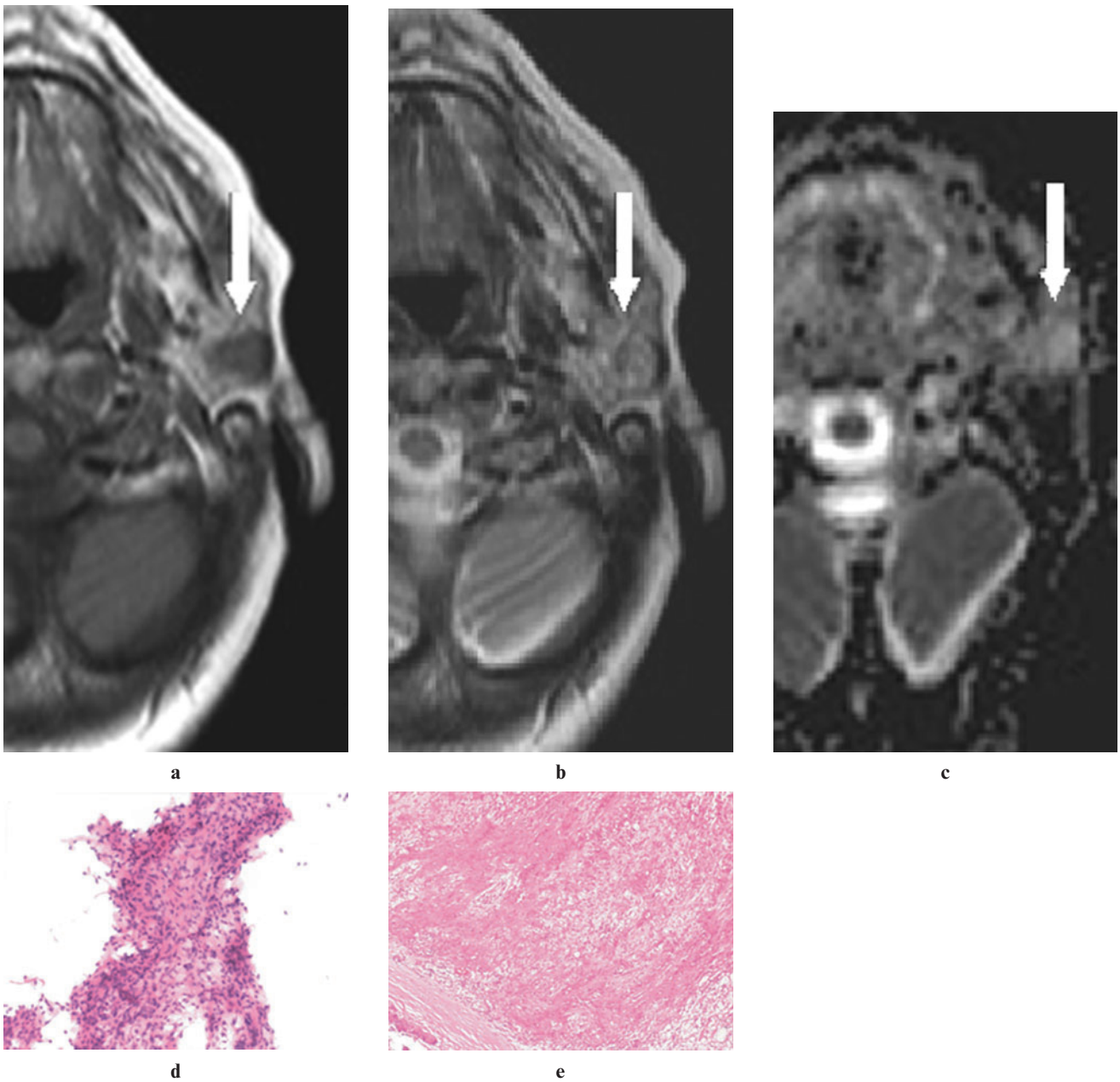

Figure 1 A pleomorphic adenoma in the superficial lobe of the left parotid gland of a 70-year-old woman. (a) An axial T1W image (500/14, TR/TE) showing a mass lesion that is hypointense (arrow) to gland parenchyma and isointense compared with muscle. (b) An axial T2W image (3800/90, TR/TE) showing a mass lesion that is isointense (arrow) with gland parenchyma and hyperintense compared with muscle. (c) An apparent diffusion coefficient (ADC) map showing a solid lesion (arrow) with high ADC (1.54×10^{-3} mm^2 s^{-1}). (d) An image of fine-needle aspiration cytology (FNAC) showing spindle-shaped mesenchymal cells intermingled with epithelial cells (haematoxylin and eosin $\times 20$ original magnification). (e) A histological section of the tumour showing biphasic appearance of pleomorphic adenoma resulting from the intimate admixture of epithelium and stroma separated from the surrounding salivary gland tissue by an intact fibrous capsule (haematoxylin and eosin $\times 10$ original magnification)

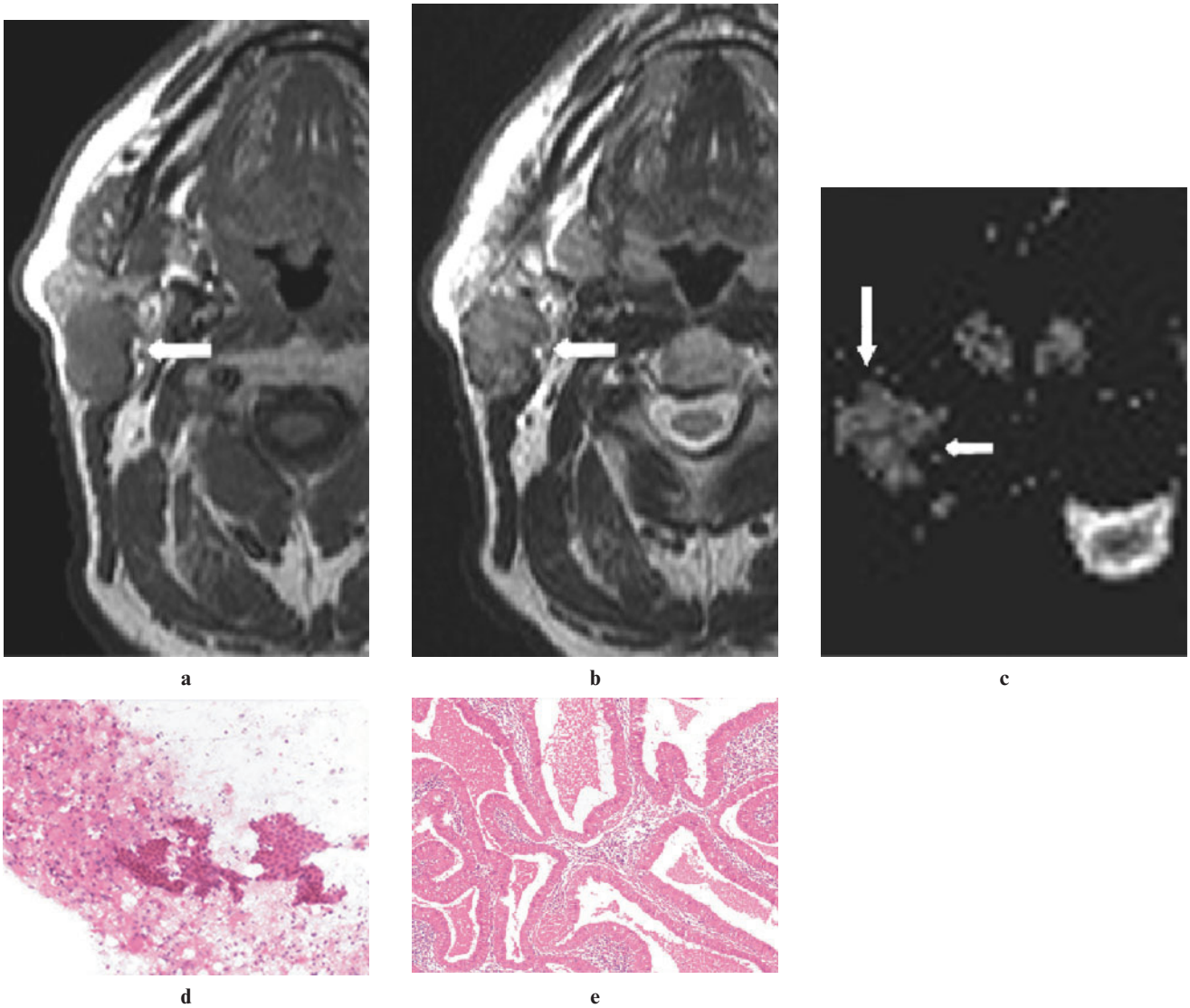

Figure 2 A Warthin tumour involving the superficial and deep lobes of the right parotid gland of a 60-year-old man. (a) An axial T1W image (500/14, TR/TE) showing a hypointense mass lesion (arrow) relative to gland parenchyma and isointense to muscle, enclosed in a rim of low signal in the posterior portion of the mass. (b) An axial T2W image (3800/90, TR/TE) showing a hypointense mass lesion (arrow), relative to the gland parenchyma and isointense to muscle, enclosed in a rim of low signal in the right lateral portion of the mass. (c) An apparent diffusion coefficient (ADC) map image showing the lesion (arrows) with low ADC of 0.62×10^{-3} mm^2 s^{-1}. (d) An image of fine-needle aspiration cytology (FNAC) showing flat sheets of oncocytic cells surrounded by lymphocytes (haematoxylin and eosin × 20 original magnification). (e) A histological section of the tumour showing lymphoid stroma surrounded by large epithelial cells with oncocytic features arranged in two layers (haematoxylin and eosin ×10 original magnification)

almost a cystic structure, had well-defined contours. 18 out of 19 benign masses (94.7%) had well-defined contours. The accuracy, sensitivity, specificity and negative and positive predictive values of conventional MRI were 96%, 80%, 100%, 94.7% and 100%, respectively (Table 1).

Statistically significant differences for measured ADC values were seen between Warthin tumours (mean, $1.02 \pm 0.13 \times 10^{-3}$ mm^2 s^{-1}) and adenomas (mean, $1.75 \pm 0.40 \times 10^{-3}$ mm^2 s^{-1}). The ADC values of carcinomas (mean, $1.31 \pm 0.16 \times 10^{-3}$ mm^2 s^{-1}) overlapped with the ADC values of benign tumours. ADC values for the two cases of lipomas were 0.08×10^{-3} mm^2 s^{-1} and 0.10×10^{-3} mm^2 s^{-1}, for haemangioma was 0.8×10^{-3} mm^2 s^{-1} and for lymphadenopathy was 0.63×10^{-3} mm^2 s^{-1}. However, the ADC values enabled the differentiation of adenomas from Warthin tumours. Therefore, MRI combined with ADC calculation was successful in determining accurate tumour typing in 18 of the 19 benign masses (94.7%).

FNAC findings

In 23 patients FNAC was performed successfully. In 3 of the 23 patients (13.0%) FNAC delivered insufficient material. Ultrasound guided FNAC was technically successful in 20 of 23 patients (87.0%). When the

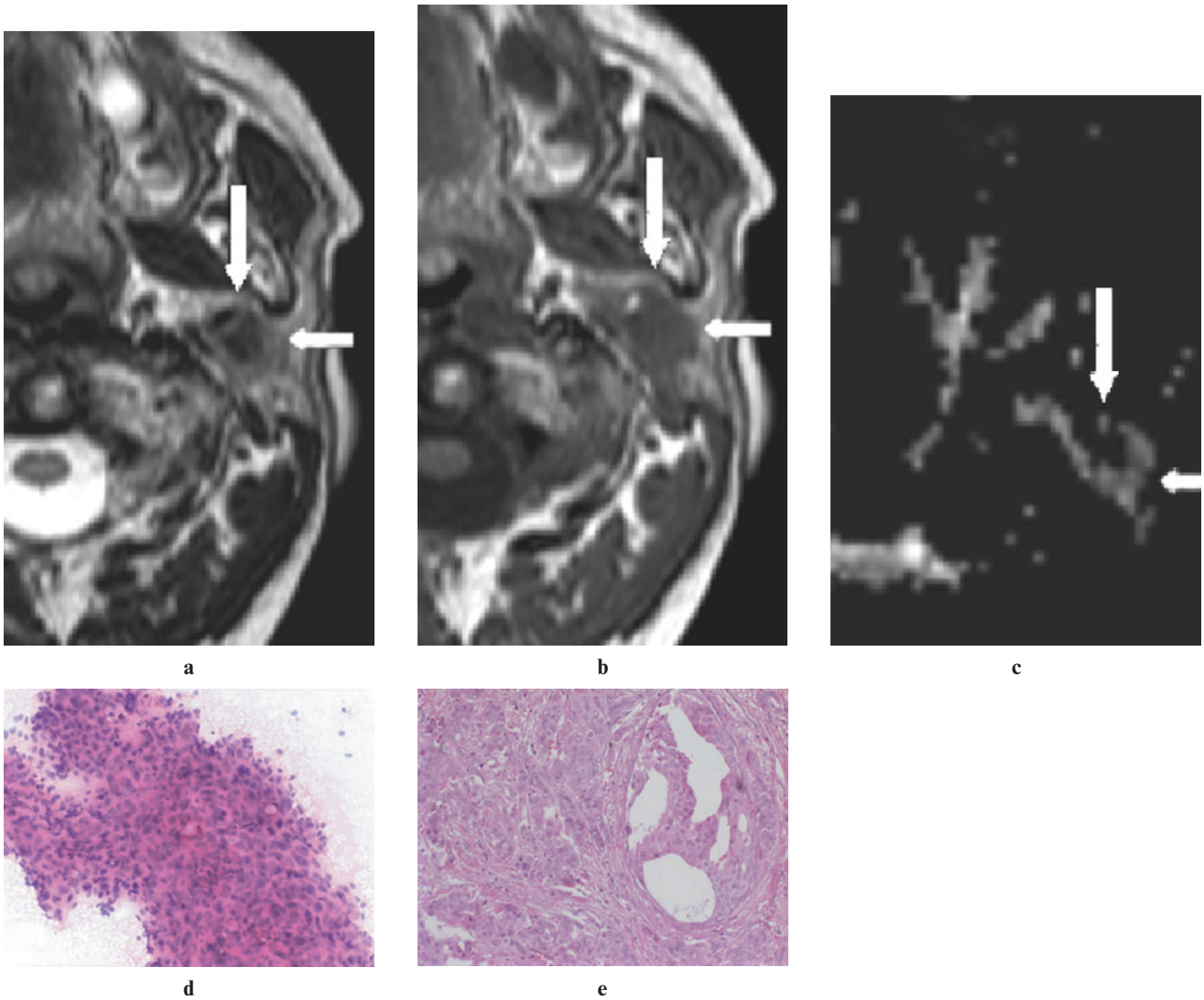

Figure 3 An adenocarcinoma located in the deep lobe of the left parotid gland of a 62-year-old man. (a) A non-contrast axial T2W image (3800/90, TR/TE) showing a heterogeneous hypointense mass (arrows) relative to the gland parenchyma. Note the ill-defined contour of the lesion. (b) A non-contrast axial T1W image (500/14, TR/TE) showing mass (arrows), hypointense to gland parenchyma. (c) An apparent diffusion coefficient (ADC) map image showing the lesion (arrows) with an intermediate ADC of 1.19×10^{-3} mm^2 s^{-1}. (d) An image of FNAC showing a cluster of pleomorphic and atypical epithelial cells (hematoxylin and eosin × 20 original magnification). (e) A histological section of the tumour showing adenocarcinoma infiltration in desmoplastic stroma (hematoxylin and eosin × 20 original magnification)

FNAC had adequate material, the accuracy, sensitivity, specificity and negative and positive predictive values were 95%, 75%, 100%, 94% and 100%, respectively (Table 1). No minor or major complications were seen during or after the procedure.

Table 1 Performance values of MRI and fine-needle aspiration cytology (FNAC) for differentiating benign from malignant parotid masses

Diagnostic performance	*MRI*	*FNAC**
Accuracy (%)	23/24 (96)	19/20 (95)
Specificity (%)	19/19 (100)	16/16 (100)
Sensitivity (%)	4/5 (80)	3/4 (75)
Negative predictive value (%)	18/19 (94.7)	16/17 (94)
Positive predictive value (%)	4/4 (100)	3/3 (100)

*Ratios for FNAC based on biopsy with adequate material

Table 1 shows the performance values of conventional MRI and FNAC for differentiating benign from malignant parotid masses. Youden's index was 0.80 for MRI and 0.75 for FNAC. The results for MRI combined with DWI *vs* FNAC in diagnosing the specific histological type of common parotid masses are compared in Table 2.

Discussion

Pre-operative diagnosis of the type of parotid mass can help the surgeon determine the most suitable surgical procedure. MRI provides morphological information of the mass and DWI provides functional information

Table 2 The results of MRI combined with diffusion-weighted imaging (DWI) *vs* fine-needle aspiration cytology (FNAC) in diagnosing the specific histological type of common parotid masses

Mass type (final histodiagnosis)	*MRI–DWI diagnosis (detected* n*)*	*FNAC diagnosis (detected* n*)*
Adenoma ($n = 6$)	6	4
Warthin tumour ($n = 8$)	8	8
Carcinoma ($n = 4$)	3	3
Lipoma ($n = 2$)	2	1
Haemangioma ($n = 1$)	1	0
Lymphadenopathy ($n = 1$)	0	1
Total ($n = 22$)	20	17

n, number of masses

related to the random water diffusion of the mass. The ADC of a parotid mass can be calculated quantitatively from DWI data.[1,2] The ADC calculation has been reported as helpful for narrowing the differential diagnosis of parotid masses.[3,4,7] Thus, the aim of this study was to evaluate the accuracy of MRI combined with DWI *vs* FNAC.

The accuracy of conventional MRI sequences in the diagnosis of common parotid masses is controversial, although some parotid tumours, such as haemangioma and lipoma, can be differentiated based on MRI signal features.[7–13,15] In the present study, one lipoma and one haemangioma which were not diagnosed by FNAC, had characteristic MRI findings (Table 2). The mass contour feature is still the most important criterion, and irregular tumour margins may still be useful in differentiating malignant parotid masses from benign masses.[8–10] Additionally, measuring ADC values for the mass may only assist in determining the specific histological type of benign parotid mass. The ADC values of carcinomas can overlap with those of Warthin tumours.[7] In the present series, all Warthin tumours and adenomas could be differentiated with the combination of conventional MRI and ADC values, whereas an overlap between carcinomas and benign lesions was noted. DWI helped in determining the specific histological type of common benign parotid masses although diagnostic accuracy did not improve by adding DWI to conventional MRI.

In this study's population no contraindications to MRI were present (for example, claustrophobia, implanted pacemakers, aneurysm clips, coronary stent or graft, or intra-auricular metallic implants), nor were any complications related to the use of contrast material. High accuracy (96%) and technical success rate (96%) were determined for MRI. Post-contrast images did not add value to the diagnosis of conventional MRI combined with DWI for parotid masses. Application of the contrast material appears unnecessary for differentiating parotid masses unless it is applied in a dynamic study.[8]

In the present study, when FNAC had adequate material, it had an accuracy (95%) similar to that of MRI. In the literature, the accuracy of FNAC ranges from 84% to 97%, which is similar to the present results. One important problem when using FNAC is that there is frequently inadequate material, which makes cytological diagnosis impossible. In the literature, non-diagnostic FNAC rates have been reported as ranging between 5.6% and 10%.[5,6] In the present study inadequate material was observed in 13% of the patients. Studies reported in the literature point out that repeating FNAC in instances of inadequate material increases the success of the procedure; repetitive FNAC procedures were not performed in this study. This may be the cause of the relatively high non-diagnostic ratio. Also, in this series, the presence of two basal cell adenomas, which are difficult to diagnose by FNAC, could have contributed to the high non-diagnostic ratio.

This study did not encounter any complications related to the biopsy procedure. Risks related to malignant cell implantation along the needle tract during FNAC of malignant parotid tumours have not been reported in the literature; however, squamous metaplasia of original oncocytic epithelium and infarct can develop in Warthin tumours after FNAC.[16] Although FNAC is a safe method, the relatively high non-diagnostic ratio in FNAC is one limitation of the method. Thus, some of the advantages of MRI, such as high technical success and valuable morphological and functional information, may increase the use of MRI in the management of this patient population.

One of the limitations of this study is that a surface coil was not used during DWI; this decreases susceptibility artefacts that are common in the neck region. Eida et al suggests that small surface coils for DWI of the neck region can be used to obtain high resolution ADC maps.[17] Another limitation of the study might be the small number of patients in this series.

In conclusion, conventional MRI and FNAC are valuable modalities for differentiating benign from malignant parotid masses. Furthermore, based on this study, when compared with FNAC, the combination of MRI and DWI with ADC calculation may have a similar diagnostic value for determining specific histological types of common parotid masses. However, the results suggest a potential role for MRI combined with DWI, including additional advantages in parotid tumour characterization, in clinical practice.

References

1. Wang J, Takashima S, Takayama F, Kawakami S, Saito A, Matsushita T, et al. Head and neck lesions: characterization with diffusion-weighted echo-planar MR imaging. *Radiology* 2001; **220**: 621–630.
2. Sumi M, Takagi Y, Uetani M, Morikawa M, Hayashi K, Kabasawa H, et al. Diffusion-weighted echoplanar MR imaging of the salivary glands. *AJR Am J Roentgenol* 2002; **178**: 959–965.
3. Motoori K, Iida Y, Nagai Y, Yamamoto S, Ueda T, Funatsu H, et al. MR imaging of salivary duct carcinoma. *AJNR Am J Neuroradiol* 2005; **26**: 1201–1206.
4. Habermann CR, Arndt C, Graessner J, Diestel L, Petersen KU, Reitmeier F, et al. Diffusion-weighted echo-planar MR imaging of primary parotid gland tumors: is a prediction of different histologic subtypes possible? *AJNR Am J Neuroradiol* 2009; **30**: 591–596.

5. Tan LG, Khoo ML. Accuracy of fine needle aspiration cytology and frozen section histopathology for lesions of the major salivary glands. *Ann Acad Med Singapore* 2006; **35**: 242–248.
6. Zbären P, Schär C, Hotz MA, Loosli H. Value of fine-needle aspiration cytology of parotid gland masses. *Laryngoscope* 2001; **111**: 1989–1992.
7. Yerli H, Agildere AM, Aydin E, Geyik E, Haberal N, Kaskati T, et al. Value of apparent diffusion coefficient calculation in the differential diagnosis of parotid gland tumors. *Acta Radiol* 2007; **48**: 980–987.
8. Alibek S, Zenk J, Bozzato A, Lell M, Grunewald M, Anders K, et al. The value of dynamic MRI studies in parotid tumors. *Acad Radiol* 2007; **14**: 701–710.
9. Takashima S, Takayama F, Wang Q, Kurozumi M, Sekiyama Y, Sone S. Parotid gland lesions: diagnosis of malignancy with MRI and flow cytometric DNA analysis and cytology in fine-needle aspiration biopsy. *Head Neck* 1999; **21**: 43–51.
10. Howlett DC, Kesse KW, Hughes DV, Sallomi DF. The role of imaging in the evaluation of parotid disease. *Clin Radiol* 2002; **57**: 692–701.
11. Ikeda K, Katoh T, Ha-Kawa SK, Iwai H, Yamashita T, Tanaka Y. The usefulness of MR in establishing the diagnosis of parotid pleomorphic adenoma. *AJNR Am J Neuroradiol* 1996; **17**: 555–559.
12. Ikeda M, Motoori K, Hanazawa T, Hanazawa T, Nagai Y, Yamamoto S, et al. Warthin tumor of the parotid gland: diagnostic value of MR imaging with histopathologic correlation. *AJNR Am J Neuroradiol* 2004; **25**: 1256–1262.
13. Yousem DM, Kraut MA, Chalian AA. Major salivary gland imaging. *Radiology* 2000; **216**: 19–29.
14. Conover WJ. Some methods based on ranks. In: Conover WJ. *Practical nonparametric statistics*. New York: John Wiley & Sons, 1980: 229–239.
15. Som PM, Biller HF. High-grade malignancies of the parotid gland: identification with MR imaging. *Radiology* 1989; **173**: 823–826.
16. Di Palma S, Simpson RH, Skálová A, Michal M. Metaplastic (infarcted) Warthin's tumour of the parotid gland: a possible consequence of fine needle aspiration biopsy. *Histopathology* 1999; **35**: 432–438.
17. Eida S, Sumi M, Sakihama N, Takahashi H, Nakamura T. Apparent diffusion coefficient mapping of salivary gland tumors: prediction of the benignancy and malignancy. *AJNR Am J Neuroradiol* 2007; **28**: 116–121.